Wavelength dependence for the photoreversal of a psoralen–DNA crosslink

3 **AUTHORS**, INCLUDING:

Yun-Bo Shi
National Institutes of Health
201 PUBLICATIONS   **7,107** CITATIONS

SEE PROFILE

John Hearst
University of California, Berkeley
52 PUBLICATIONS   **1,367** CITATIONS

SEE PROFILE

Wavelength Dependence for the Photoreversal of a Psoralen–DNA Cross-Link[†]

George D. Cimino,[‡] Yun-bo Shi, and John E. Hearst*

Department of Chemistry, University of California, Berkeley, California 94720

Received October 15, 1985; Revised Manuscript Received January 9, 1986

ABSTRACT: We report an action spectrum for the photoreversal of a psoralen cross-link joining two self-complementary DNA oligonucleotides. The cross-link was formed between two thymines (T) on opposite strands of the DNA oligomers and 4'-(hydroxymethyl)-4,5',8-trimethylpsoralen (HMT). For comparison, we also present an action spectrum for the photoreversal of the isolated diadduct T–HMT–T. The wavelength dependence for the diadduct photoreversal parallels its absorption spectrum. Both the diadduct and the cross-linked DNA can be photoreversed by exposure to light with wavelengths between 240 and 313 nm. We did not observe photoreversal at 334 nm or above. At least two distinct absorption bands appear to contribute to photoreversal. We measured a quantum yield of 0.16 for photoreversal of the isolated diadduct at wavelengths between 240 and 266 nm. For wavelengths above 280 nm, the quantum yield is 0.30. We also observed a preferential photoreversal at the furan end of the psoralen in the T–HMT–T diadduct. In contrast, the cross-linked DNA oligonucleotides preferentially photoreversed at the pyrone end of the psoralen adduct. The rate constant for photoreversal of the cross-linked DNA is larger than that for the isolated diadduct at wavelengths below 300 nm.

Psoralens are a class of planar, three-ring heterocyclic compounds (furocoumarins). The chemical properties of several natural and synthetic psoralens have been studied for over 2 decades [for reviews, see Cimino et al. (1985), Song & Tapley (1979), and Parson (1980)]. These molecules have the ability to intercalate between the bases of a double-helical nceic acid (Isaacs et al., 1977, 1982). Upon exposure to long-wavelength UV radiation (320–400 nm), a limited and well-characterized set of covalent adducts is formed between psoralens and pyrimidine bases (Straub et al., 1981; Kanne et al., 1982a,b). Covalent cycloaddition occurs between the 5,6 double bond of pyrimidine bases and either the 3,4 double bond of a psoralen, which forms a "pyrone-side monoadduct", or the 4',5' double bond of a psoralen, which yields a "furan-side monoadduct". Psoralens react primarily with thymidine in DNA and uridine in RNA, although a minor reaction with cytosine also occurs (Turner & Noller, 1983; Garrett-Wheeler et al. 1984). When a psoralen molecule is intercalated between adjacent pyrimidine bases on opposite strands of a double-helical segment of DNA or RNA, a diadduct can be photochemically induced which covalently cross-links the two nucleic acid strands. The formation of the diadduct is a polar reaction. The furan-side monoadduct must be formed initially. Continued irradiation into the absorption band of this monoadduct (320–380 nm) results in cycloaddition at the pyrone end of the psoralen if it is positioned in a cross-linkable site (Kanne et al., 1982; Gasparro et al., 1984). Cross-links and monoadducts are both photoreversable by exposure to shorter wavelength UV light (typically 254 nm). The exact structure of a monoadduct is known from X-ray crystallographic studies (Peckler et al. 1982), and a theoretical molecular structure of the diadduct in a DNA helix has recently been proposed (Pearlman et al., 1985).

This thorough understanding of the chemistry and photochemistry of psoralens has resulted in their widespread use in the medical and biological fields. These compounds are used in the treatment of psoriasis and vitiligo (Fitzpatrick et al., 1982). Psoralens plus UV light (320–400 nm) have both lethal and mutagenic effect in cells (Fujita, 1984; Cassier et al., 1984) and form nucleic acid lesions that are recognized by repair systems (Ben-Hur & Song, 1984; Saffran & Cantor, 1984). Psoralens are also used widely as probes to study nucleic acid structure and function [for a review, see Cimino et al. (1985)]. Procedures have been developed utilizing psoralens to map secondary and tertiary structure in large RNA molecules (Thompson et al., 1983). These procedures employ both the cross-linking and photoreversal reactions of psoralen molecules. Relatively little is known about the wavelength dependency of these photoreactions. Gasparro et al. (1984) have recently reported the action spectrum for the cross-linking of pBR322 DNA. They observed that the wavelength dependency for cross-link formation correlates with the absorption spectrum of the furan-side monoadduct.

In this paper we report an action spectrum for the photoreversal of an isolated diadduct between 4'-(hydroxymethyl)-4,5',8-trimethylpsoralen (HMT)[1] and thymidine (T–HMT–T) and an action spectrum for the photoreversal of the same T–HMT–T diadduct in the double-stranded KpnI linker 5'-GGGTACCC-3' (a DNA–HMT cross-link). Some differences were observed which we interpret to be the result of the positioning of a diadduct in a nucleic acid helix. We also show that the formation of furan-side monoadduct and pyrone-side monoadduct from the photoreversal of a diadduct is dependent on the irradiation wavelength and the pH of the photoreversal solution. The incorporation of the diadduct into a DNA helix also has a dramatic effect on the formation of one monoadducted DNA vs. the other upon photoreversal.

---

[1] Abbreviations: HMT, 4'-(hydroxymethyl)-4,5',8-trimethylpsoralen; KpnI linker, 5'-GGGTACCC-3'; EtOH, ethanol; ATP, adenosine triphosphate; EDTA, ethylenediaminetetraacetic acid; XL, psoralen cross-linked KpnI DNA; M_{Py}, pyrone-side psoralen monoadducted oligonucleotide; M_{Fu}, furan-side psoralen monoadducted oligonucleotide; f, unreacted KpnI DNA; T–HMT–T, thymidine–HMT–thymidine diadduct; T–HMT–C, thymidine–HMT–cytosine diadduct; Tris-HCl, tris(hydroxymethyl)aminomethane hydrochloride; HPLC, high-performance liquid chromatography.
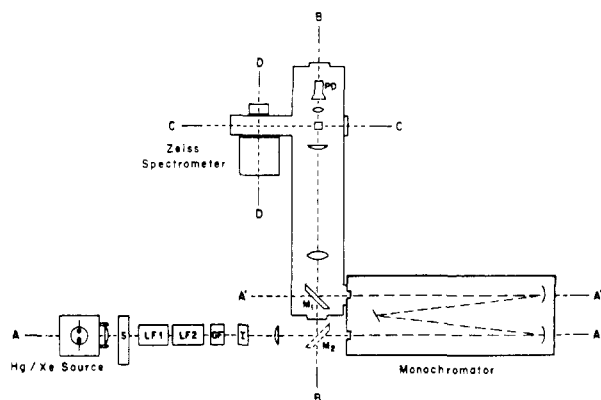
FIGURE 1: Schematics of the irradiation apparatus: The apparatus is designed to produce either high-intensity monochromatic light or very high intensity broad-band light for preparative purposes. Light from an arc source (2.2-kW Xe or 2.5-kW Hg) is passed through a shutter (S) which is operated by an external clock. Broad-band radiation is selected by a combination of liquid filters (LF1 and LF2). Glass filters (GF) provide order sorting capacity when monochromatic light is desired and are also used as cutoff filters. An iris diaphram (I) is used to adjust the intensity. Cuvettes, positioned at the intersection of axes B and C, can be exposed to either broad-band or monochromatic radiation. When monochromatic radiation is desired, light enters the monochromator (Model CT-103, One-Meter Spectrometer, Interactive Technology, Los Gatos, CA) along axis A and emerges along axis A'. Mirror M1 deflects the monochromatic beam along axis B. A series of lenses focus the beam at the intersection of axes B and C. A photodiode (PD, Model HUV-4000B, EG&G Inc., Salem, MA), positioned behind a diffuser (Oriel UV Diffuser 4812), continuously monitors the intensity of the beam. When broad-band radiation is desired, Mirror M1 is removed and a second morror (M2) is placed at the intersection of axes A and B. Mirror M2 deflects the beam from axis A to axis B. The beam is then focused onto the sample and monitored as described. Mirror M2 can also deflect the beam perpendicular to the plane described by axes A and B. This capability permits irradiation of large volumes of solution, or cells attached to a flask or Petri dish. The thermoregulated cuvette holder accepts a standard 1 cm × 1 cm cuvette or a 2.5 cm × 2.5 cm cuvette, allowing volumes of up to 30 mL to be easily irradiated. The curvette holder, which includes a magnetic stirrer, is mounted on a translatable rail. This holder is positioned at the intersection of axes B and C during irradiations. By translating the holder along axis C, a sample can be positioned in the optical beam of a Zeiss spectrometer. Any optical density changes that occur during irradiations are easily monitored without exposure to room light. This capability is desired when precise dosimetry is necessary. A viewing port along axis C in the side of the spectrometer box permits fluorescence measurements.

MATERIALS AND METHODS

Materials. HMT and [³H]HMT were gifts from HRI Associates Inc. (Emeryville, CA). The oligonucleotide, 5'-GGGTACCC-3' (*Kpn*I linker), was either purchased from New England Biolabs or synthesized on an automated DNA synthesizer (SAM ONE DNA Synthesizer, Biosearch). [γ-³²P]ATP was obtained from Amersham. T4 polynucleotide kinase was bought from Bethesda Research Laboratories. Poly(dA-T), DNase II, bacterial alkaline phosphatase, and phosphodiesterase II were obtained from Sigma. Sephadex G-10 was purchased from Pharmacia Fine Chemicals. 1,10-Phenanthroline was bought from Aldrich Chemical Co. Potassium ferric oxalate was purchased from ICN Pharmaceuticals, Inc. All the chemicals were used without further purification.

Irradiations. (*A*) *Broad-Band Irradiation.* Samples were irradiated with the apparatus described in Figure 1. Infrared radiation was removed by a water filter (9 cm) at position LF1. An aqueous solution of cobaltous nitrate (1.7% cobaltous nitrate, 2% sodium chloride, 9-cm path length) was placed at LF2, providing a band of light in the range 320–380 nm

(Hearst et al, 1984). A Pyrex filter was required in front of LF2 to prevent photodegradation of the cobaltous nitrate solution by short-wavelength radiation. The intensity of the beam was measured with a Blackray longwave (300–400 nm) ultraviolet meter (Model J221, San Gabriel, CA). At the focal point, the beam had a diameter of 2.1 cm and a maximum intensity of 1 W/cm².

(*B*) *Monochromatic Irradiation.* Monochromatic light was selected as described in Figure 1. The optical path contained only a water filter at position LF1. Positions LF2 and GF were both unoccupied in order to pass short-wavelength UV light. For irradiations above 313 nm, a Pyrex filter was placed at the exit of the monochromator to cutoff short-wave scattered radiation emitted from the monochromator. The bandwidth for all monochromatic irradiations was maintained constant at 2.5 nm. Monochromatic radiation was continuously monitored with an in-line photodiode. This photodiode was calibrated by actinometry with $K_3Fe(C_2O_4)_3$ (Paul de Mayo & Shizuk, 1976). The amount of Fe^{2+} produced was determined by the absorption of the complex formed between Fe^{2+} and 1,10-phenanthroline at 510 nm. The maximum light intensity at 365 nm of this instrument with a 2.5-kW Hg/Xe lamp is 10^{16} photons/s. The irradiation intensities used in the experiments varied between 10^{14} and 10^{16} photons/s.

Preparation of DNA–HMT Cross-Link. A total of 25 μg of *Kpn*I linker DNA was 5'-end labeled with [γ-³²P]ATP and T4 polynucleotide kinase according to standard procedures (Maniatis et al., 1982). A solution (140 μL) containing the *Kpn*I linker, 0.9 mCi of [γ-³²P]ATP (3000 Ci/mmol), 14 μL of 10X linker kinase buffer (700 mM Tris-HCl, 100 mM $MgCl_2$, and 50 mM dithiothreitol, pH 7.6), and 10 units of T4 polynucleotide kinase was incubated at 37 °C for 30 min. Ten additional units of the kinase was added to the solution which was then incubated for another 30 min. This reaction was subsequently chased with cold ATP by adding 21 μL of 10 mM ATP, 3 μL of 10X linker kinase buffer, and 10 additional units of the kinase and incubating again at 37 °C for 30 min. Unreacted ATP was removed by chromatography on a Sephadex G-10 column, which was equilibrated with irradiation buffer (pH 7.6, 50 mM Tris-HCl, 0.1 mM EDTA, 75 mM NaCl, and 3 mM $MgCl_2$). A total of 5 μL of 2.5 mM HMT in EtOH was then added to the labeled DNA solution (160 μL). This solution was irradiated for 3 min at 4 °C with broad-band light in a 1.5-mL Eppendorf tube. HMT addition and subsequent irradiation were repeated 3 times. Unreacted and photodamaged HMT were removed by extracting twice with chloroform–isoamyl alcohol (24:1 v/v) and twice with water-saturated ether. The DNA was then EtOH-precipitated, washed, and electrophoresed on a 20% polyacrylamide–7 M urea gel (20 cm × 40 cm × 0.08 cm). The cross-link band was located by autoradiography, excised, and eluted from the gel into a solution of 50 mM NaCl–1 mM EDTA solution. The cross-link was further purified by EtOH precipitation and disolved in 200 μL of TE buffer (pH 7.6, 10 mM Tris-HCl and 1 mM EDTA), and stored at -20 °C.

Preparation of HMT–Thymidine Diadduct. A total of 45 μL of [³H]HMT solution (2.5 μg/μL in EtOH, 4.4 Ci/mmol) was added to 3 mL of 500 μg/mL poly(dA-T) in 10 mM Tris-HCl and 1 mM EDTA, pH 7.5, and the mixture was irradiated with broad-band light for 8 min at 4 °C. Another 45 μL of the concentrated HMT stock solution was added, and the mixture was reirradiated for an additional 6 min. The photoreacted poly(dA-T) was purified by extracting twice with chloroform–isoamyl alcohol (24:1 v/v) and twice with water-saturated ether and then by EtOH precipitation. Fi-
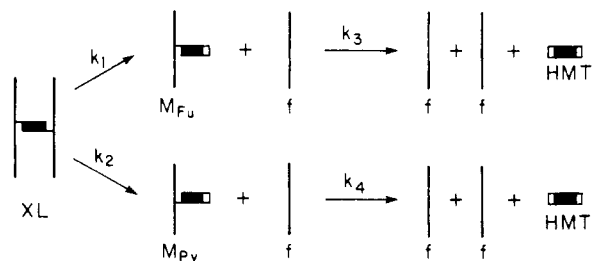
FIGURE 2: Model for photoreversal of the diadduct or cross-link under conditions where free KpnI linker is denatured.

nally, the precipitate was digested sequentially with DNase II, phosphodiesterase II, and alkaline phosphatase as previously described (Kanne et al., 1982b). The diadduct was isolated by loading the digest on a 10 mm × 25 cm reverse phase (C_{18}) HPLC column (Ultrasphere ODS, Altex-Beckman, Berkeley, CA) and eluting with a linear 10 mM KH$_2$PO$_4$(pH 2.2)–CH$_3$OH gradient over a period of 80 min (1 fraction/1 min). The purified diadduct (fraction 29) was vacuum dried without prior neutralization and dissolved back in an acetate buffer. The diadduct was then stored at −20 °C in 150 mM NaOAc and 27 mM KH$_2$PO$_4$ (pH 5.0), which includes the PO$_4^{3-}$ or KH$_2$PO$_4$ from the HPLC gradient.

Photoreversals. The DNA–HMT cross-link (5 × 10^{-9} M) was photoreversed in a 1-cm path-length quartz cuvette in one-tenth TE buffer (pH 7.5, 1 mM Tris-HCl, 0.1 mM EDTA, and ca. 2 mM NaCl) at room temperature with monochromatic light. During photoreversal, the samples were continuously stirred under a N$_2$ atmosphere. After photoreversal, the samples were dried without heating in a Speedvac concentrator (Savant Intrument Inc.), dissolved in 7 M urea, 0.05% bromophenol blue, and 0.05% xylene cyanol FF solution, and then electrophoresed on a 20% polyacrylamide–7 M urea gel. Band positions of the cross-linked, monoadducted, and free oligonucleotides were located by autoradiography (Gamper et al., 1984), excised, and quantified by Cerenkov counting with a Beckman LS-230 liquid scintillation counter.

The HMT–thymidine diadduct (1.3 × 10^{-7} M) was photoreversed with monochromatic light in a stirred cuvette in 20 mM NaOAc and 0.4 mM KH$_2$PO$_4$, pH 5.45, solution at room temperature. The photoreversed samples were run through the reverse-phase HPLC column with a linear KH$_2$PO$_4$–CH$_3$OH gradient. The diadduct, monoadducts, and free HMT were identified by their retention time on the column as characterized by Kanne et al. (1982a) and quantified by ^{3}H scintillation counting. The diadduct, furan-side monoadduct, pyrone-side monoadduct, and HMT eluted at fractions 29, 39, 50, and 55, respectively.

Analysis of the Photoreversal Kinetics. Under denaturing conditions complete photoreversal of the cross-link is a two-step reaction (see Figure 2). The initial photoreversal of a cross-link (XL) yields two distinct monoadducted oligonucleotides. An oligonucleotide with a furan-side monoadduct (M_{Fu}) is formed when photoreversal occurs at the pyrone end of the HMT, and an oligonucleotide with a pyrone-side monoadduct (M_{Py}) is formed when photoreversal occurs at the furan end of the HMT. The rate constants for the two processes are k_1 and k_2, respectively. The second step is the photoreversal of the monoadducted oligonucleotides to produce free DNA (f) and free HMT. The rate equations for these reactions are

$$dC/dt = -a[k_1 + k_2]C \qquad (1)$$

$$dC_{Fu}/dt = ak_1C - ak_3C_{Fu} \qquad (2)$$

$$dC_{Py}/dt = ak_2C - ak_4C_{Py} \qquad (3)$$

$$dC_f/dt = a[k_1 + k_2]C + ak_3C_{Fu} + ak_4C_{Py} \qquad (4)$$

where a is a constant that is defined as $a = I_0l/(VN_0)$, in which V is the reaction volume (liters), N_0 is Avogadro's number, I_0 is the photon intensity (photons per second), and l is the path length (centimeters); C, C_{Fu}, C_{Py}, and C_f are the concentrations in moles per liter of XL, M_{Fu}, M_{Py}, and f, respectively; k_i ($i = 1, 2, 3, 4$) are the corresponding rate constants (liters per einstein centimeter).

The solutions to these equations at initial conditions $C_f = C_{Fu} = C_{Py} = 0$ and $C = C^0$ are

$$C = C^0 \exp[-a(k_1 + k_2)t] \qquad (5)$$

$$C_{Fu} = [k_1C^0/(k_1 + k_2 - k_3)] \exp(-ak_3t) - \\ [k_1C^0/(k_1 + k_2 - k_3)] \exp[-a(k_1 + k_2)t] \quad (6)$$

$$C_{Py} = [k_2C^0/(k_1 + k_2 - k_4)] \exp(-ak_4t) - \\ [k_2C^0/(k_1 + k_2 - k_4)] \exp[-a(k_1 + k_2)t] \quad (7)$$

$$C_f = C^0\{1 - \exp[-a(k_1 + k_2)]\} + \\ \{k_2k_4C^0/[(k_1 + k_2)(k_1 + k_2 - k_4)]\} \times \\ \{\exp[-a(k_1 + k_2)t] - 1\} + \{k_1C^0/(k_1 + k_2 - k_3)\}\{1 - \\ \exp[-ak_3t]\} + \{k_2C^0/(k_1 + k_2 - k_4)\}\{1 - \exp[-ak_4t]\} + \\ \{k_1k_3C^0/[(k_1 + k_2)(k_1 + k_2 - k_3)]\}\{\exp[-a(k_1 + k_2)t] - 1\} \\ (8)$$

At low concentrations of the cross-link, the rate constants k_i ($i = 1, 2, 3, 4$) are related to the molecular properties of the reactant molecules in a simple manner:

$$k_i = 2.303\epsilon_i\phi_i \qquad (9)$$

where ϵ_i and ϕ_i are the corresponding extinction coefficients (liters per mole centimeter) and quantum yields (see paragraph at end of paper regarding supplementary material).

When photoreversal is limited such that the second step is negligible, the following equation also holds true:

$$C_{Fu}/C_{Py} = k_1/k_2 \qquad (10)$$

The analysis presented here is applicable to the diadduct photoreversal with replacements of free thymidine for free DNA as the meaning of f, monoadducts for monoadducted oligonucleotides as the meanings of M_{Fu} and M_{Py}, and diadduct for cross-link as the meaning of XL.

RESULTS

Identification of the Site of HMT Cross-Linkage in DNA. There are two types of cross-linking sites in the double-stranded KpnI linker. These are T–HMT–T and T–HMT–C. In order to identify precisely the cross-linking site in the isolated cross-linked molecules, DNA-[^{3}H]HMT cross-link, generated as described under Materials and Methods, was digested to nucleosides by sequential treatment with DNase II, phosphodiesterase II, and alkaline phosphatase. The digest was analyzed by HPLC. Ninety-seven percent of the ^{3}H counts eluted in the peak corresponding to T–HMT–T diadduct. The cross-lining site is, therefore, the thymidine base on each KpnI linker of the cross-link. Monoadducts of HMT with cytidine were not observed in the digest. Monoadducts of HMT with thymidine were observed at a level of less than 3% of the total ^{3}H recovered and may have been produced during the enzymatic digestions as a result of lengthy exposure to room and window lighting. These results are in agreement with those of Gamper et al. (1984).

Photoreversal of the DNA–HMT Cross-Link. The DNA–HMT cross-link was photoreversed under denaturing conditions by irradiating with monochromatic light. The photoreversal products were separated by polyacrylamide gel elec-
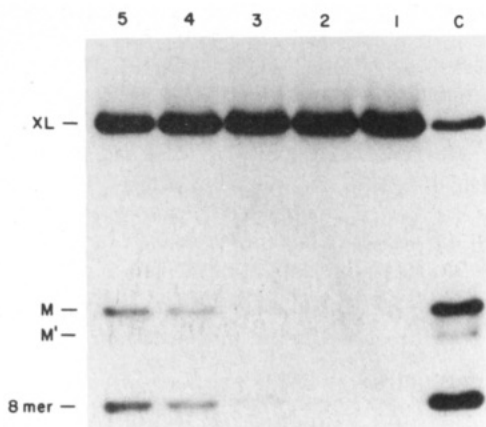
FIGURE 3: Photoreversal of the cross-link at 296 nm. Sample C is a control which was exposed to 254-nm light from a low-pressure 40-W germicidal lamp (3 min at a distance of about 6 cm). Sample 1 is a dark control. Samples 2–5 were photoreversed for 15, 75, 300, and 520 s, respectively. The light intensity was 3.80×10^{14} photons/s. $V = 750$ μL, $l = 1$ cm, and pH 7.5. XL is the cross-link band, M is the monoadducted DNA band, M' is discussed in the text, and 8-mer is the free KpnI linker band.
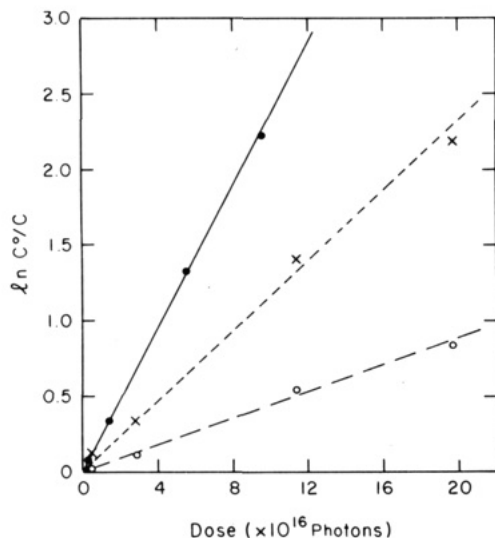

FIGURE 5: Action spectra for the photoreversal of the DNA–HMT cross-link and T–HMT–T diadduct. At 334 nm, $k_1 + k_2$ is equal to 0 for both the cross-link and diadduct.

FIGURE 4: ln (C^0/C) vs. irradiation dose for the photoreversal of the DNA–HMT cross-link at three different wavelengths. (—) Photoreversal at 249 nm, $I_0 = 1.85 \times 10^{14}$ photons/s; (- - -) photoreversal at 266 nm, $I_0 = 2.68 \times 10^{14}$ photons/s; (– – –) photoreversal at 288 nm, $I_0 = 3.80 \times 10^{14}$ photons/s. $V = 750$ μL, $l = 1$ cm, and pH 7.5.

FIGURE 6: ln (C^0/C) vs. irradiation dose for the photoreversal of the T–HMT–T diadduct at three different wavelengths. (—) Photoreversal at 249 nm, $I_0 = 2.70 \times 10^{14}$ photons/s; (- - -) photoreversal at 266 n, $I_0 = 1.08 \times 10^{14}$ photons/s; (– – –) photoreversal at 288 nm, $I_0 = 2.42 \times 10^{14}$ photons/s. $V = 1500$ μL, $l = 1$ cm, and pH 5.5.

trophoresis. An autoradiogram of a time course of the photoreversal is shown in Figure 3. With increasing exposure to light, the concentration of the cross-link decreased as the concentrations of the free KpnI linker and the monoadducted oligonucleotides increased. The band labeled as M' is tentatively identified as the pyrone-ring-opened form of the pyrone-side monoadducted oligonucleotide. A detailed discussion of this band is given in a later section. In order to determine the concentrations of each product, the bands were excised and counted. Under the electrophoretic conditions used, the two types of monoadducted oligonucleotides M_{Fu} and M_{Py} were not resolved. Therefore, only the sum of $k_1 + k_2$ could be determined. These values were obtained by plotting ln (C^0/C) vs. the irradiation dose. The plots of ln (C^0/C) vs. dose for the photoreversal at three wavelengths are shown in Figure 4. The rate constant $k_1 + k_2$ was calculated from the slope of the straight lines. The experiments were repeated at different wavelengths from 240 to 365 nm. The final results are shown in the action spectrum in Figure 5. At $\lambda \geq 334$ nm, there is no detectable photoreversal.
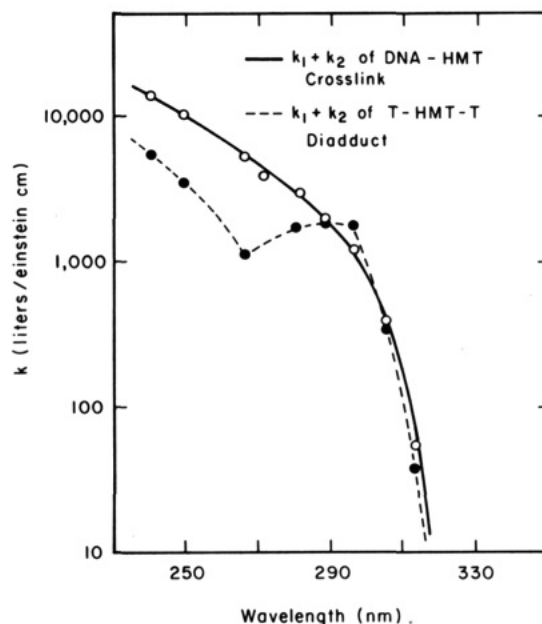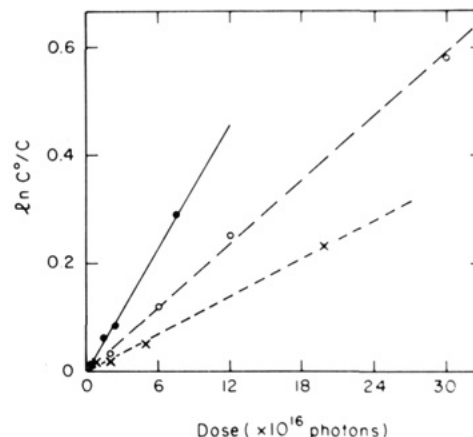
The reciprocity of photoreversal was confirmed by exposing several identical samples to a constant dose (2.70×10^{16} photons) at 296 nm. The dose rate seen by each sample was varied up to a factor of 4. The irradiation times were changed correspondingly to maintain the constant dose. All irradiated samples photoreversed to an identical extent. Thus, under our experimental conditions, the photoreversal reaction is dependent only on the total irradiation dose and not on the light intensity. The initial photoreversal to give monoadducted oligonucleotides is a one photon process.

Photoreversal of T–HMT–T Diadduct. The T–HMT–T diadduct was photoreversed at pH 5.5. The products were analyzed by HPLC. The amounts of diadduct, furan-side monoadduct, pyrone-side monoadduct, and free HMT were determined by ^{3}H scintillation counting. These data were analyzed similarly to the cross-link photoreversal data. The plots of ln (C^0/C) vs. dose for the photoreversal at three wavelengths are shown in Figure 6. The value of $k_1 + k_2$ is calculated from the slope of the line. The individual values of k_1 and k_2 can also be obtained from the sum of $k_1 + k_2$ and the use of eq 10. The experiments were repeated from 240
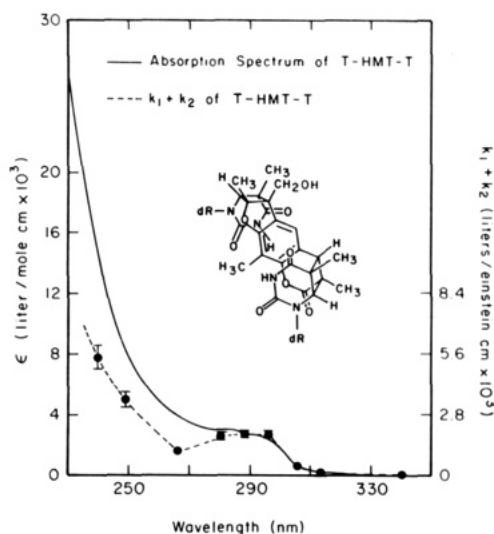
FIGURE 7: Extinction spectrum and the action spectrum of the T–HMT–T diadduct. The absorption of the diadduct was measured with a Cary 118 spectrophotometer in a solution (pH 5.5) or 110 mM NaOAc and 25 mM Na_2HPO_4, and the concentration of the diadduct was determined by ^3H scintillation counting.

FIGURE 8: Acidic and basic incubation of the furan-side monoadducted DNA (M_{Fu}) and pyrone-side monoadducted DNA (M_{Py}). The starting material of the right lane of each pair is M_{Fu}, and that of the left lane is M_{Py}. C denotes starting materials before incubation. These samples were excised as single bands from a preparative gel, eluted at pH 7, 37 °C, and kept at 4 °C for several days before use. The sample set labeled pH = 10.0 was incubated at 60 °C for 2 h in 20 mM borate buffer, pH 10.0. The sample set labeled pH = 4.0 was incubated at 60 °C for 2 h in 20 mM succinate buffer, pH 4.0.

Table I: k_2/k_1 Ratio for the Photoreversal of T–HMT–T Diadduct and DNA–HMT Cross-Link

		wavelength (nm)		
	pH	249	288	313
T–HMT–T	5.5	2.5 ± 0.5	4.5 ± 0.9	4.5 ± 0.9
diadduct	7.5	2.5 ± 0.5	≥ 20	≥ 20
	8.0	2.8 ± 0.6	≥ 20	≥ 20
DNA–HMT	7.5	0.42 ± 0.11	0.42 ± 0.11	0.28 ± 0.04
cross-link	10.0	0.68 ± 0.02	0.79 ± 0.05	1.2 ± 0.03
	12.0	6.3 ± 1.3	4.9 ± 1.0	4.7 ± 0.95

to 334 nm to obtain the action spectrum for the photoreversal of the diadduct. These results are also shown in Figure 5. There is no detectable photoreversal at 334 nm.

The extinction spectrum of the isolated diadduct is plotted together with the action spectrum for photoreversal of the diadduct in Figure 7. The extinction spectrum was determined by measuring the absorption spectrum of a sample of the HPLC purified diadduct on a Cary 118 spectrophotometer at room temperature. The concentration of this same sample of diadduct was then calculated by measuring the tritium decay from the [^3H]HMT in the diadduct. By use of the data in Figure 7, the total quantum yield for the photoreversal of the diadduct can be estimated. The quantum yield is 0.16 ± 0.04 at wavelengths between 240 and 266 nm and 0.30 ± 0.04 at wavelengths between 280 and 305 nm. These results indicate that two distinct absorption bands are contributing to photoreversal. For wavelengths below 280 nm, the major contribution is probably from excitation of the adducted pyrimidines. Above 280 nm, the benzene ring remaining in the adducted psoralen may be contributing to photoreversal.

Origin of M′. To investigate the origin of M′, tritium-labeled DNA–HMT cross-link was photoreversed by exposure to 254-nm light from a low-pressure germicidal lamp and electrophoresed on a 20% polyacrylamide–7 M urea gel. In order to resolve the two types of monoadducted oligonucleotides, a thinner gel was used (0.4 mm compared to 0.8 mm previously used). An autoradiogram of the gel showed that, in addition to the M′ band, two distinct bands at the monoadducted oligonucleotide position could be resolved (for an example, see Figure 8). These two bands were isolated, digested to nucleosides, and then analyzed by HPLC. The HPLC results showed that the faster moving band, M_{Fu}, contained a furan-side monoadduct, and the slower moving band, M_{Py}, contained a pyrone-side monoadduct. The origin of M′ was identified by incubating samples of M_{Fu} and M_{Py} in acidic and basic solutions at 60 °C for 2 h. These samples were then electrophoresed again on a thin polyacrylamide gel. The autoradiogram of this gel shown in Figure 8 indicates that M′ and M_{Py} are interconvertible by varying the pH of the solution. There was no conversion between M′ and M_{Fu}. It has been reported (Kanne et al., 1982a) that the pyrone ring of the diadduct can be opened in nonacidic solutions at pos-
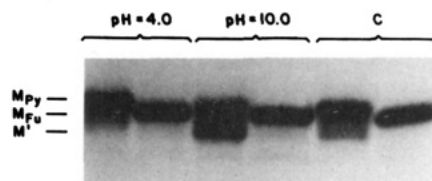
itions 1 and 2 of the psoralen moiety to yield a carboxylic group. A pyrone-ring-opened adduct in a DNA oligonucleotide would carry an additional negative charge on the carboxylic group at pH 8.5 during gel electrophoresis and, therefore, would migrate faster. On the basis of these results, it is likely that M′ is the pyrone-ring-opened form of the pyrone-side monoadducted oligonucleotide. The nature of the resolution of the two types of monoadducted oligonucleotides, M_{Fu} and M_{Py}, under refined electrophoretic conditions is not understood at this time. Possible explanations include different degrees of hydration and differences in steric hindrance.

Factors Affecting Photoreversal at the Pyrone vs. Furan Ends of a Psoralen Diadduct or Cross-Link. The initial photoreversal reaction of a diadduct yields either a furan-side monoadduct or a pyrone-side monoadduct and free thymidine. Similarly, the initial photoreversal of a cross-linked DNA produces either M_{Fu} or M_{Py} and a free strand of DNA. While the data for the photoreversal action spectrum of the diadduct were collected, it was observed that photoreversal is not symmetric. Pyrone-side monoadduct is obtained in higher yield compared to furan-side monoadduct. Furthermore, it was also observed that the ratio of pyrone-side monoadduct to furan-side monoadduct varies with both the wavelength of incident light and the pH of the photoreversal solution. Consequently, the ratio of the rate of pyrone-side monoadduct production to the rate of furan-side monoadduct production (k_2/k_1) was examined further. Solutions of the diadduct at different pH values (range from 2.2 to 8.0) were incubated at 37 °C for 1 h and then photoreversed. After photoreversal, the samples were brought back to pH 2.2 for 30 min to ensure ring closure of the pyrone-side adduct and the diadduct. These samples were then analyzed by HPLC. The ratio of k_2/k_1 was calculated according to eq 10 at several different wavelengths. In Table I, it is shown that k_2/k_1 varies with wavelength at pH 5.5 (20 mM NaOAc). The k_2/k_1 ratio at 249 nm is 2.5 compared to 4.5 for wavelengths above 280 nm. This result also supports the notion that there are two distinct photoreversal bands in the region of 240–313 nm. Both bands appear to preferentially effect photoreversal at the furan end of a diadduct. The longer wavelength band ($\lambda \geq 280$ nm) is about 2 times more effective in photoreversal at the furan end of the diadduct than the

shorter wavelength band ($\lambda < 280$ nm). Similar k_2/k_1 ratios were obtained when photoreversal was done at pH 2.2 (10 mM KH_2PO_4; data not shown). The pyrone ring of a pyrone-side monoadduct and diadduct is closed at pH 2.2. Since identical k_2/k_1 ratios were obtained at pH 2.2 and 5.5, it is believed that only the closed form of the diadduct is present at pH 5.5. At pH 7.5 (one-tenth TE buffer) the k_2/k_1 ratio is greater than 20 at 288 and 313 nm. Further increase of pH to 8.0 (10 mM Tris-HCl and 1 mM EDTA) did not change the ratio. On the basis of these observations, it is proposed that the pyrone-ring-opened form of the diadduct is the predominant form at pH 7.5 or above and that the photoreversal of the pyrone-ring-opened diadduct at the longer wavelengths (288 and 313 nm) yields only pyrone-side monoadduct because of the loss of the conjugation of the pyrone ring to the benzene ring. Prolonged irradiation at longer wavelengths did not produce free HMT at pH 7.5 or 8.0, suggesting the open form of a pyrone-side monoadduct is the terminal product of the photoreversal of a diadduct at these wavelengths. At 249 nm, however, the k_2/k_1 ratio does not change with pH. This suggests that the photoreversal at this wavelength is caused predominantly by the absorption of the remaining thymidine group in the diadduct, and consequently, it is independent of the pyrone ring opening.

Similar experiments were performed with the cross-link by electrophoresis in a thin gel (0.4 mm) to resolve the two types of monoadducted oligonucleotides. The k_2/k_1 ratio was calculated according to eq 10 with the assumption that M' is the pyrone-ring-opened form of the pyrone-side monoadducted DNA. At pH 7.5, the k_2/k_1 ratio is again wavelength dependent. In contrast to diadduct photoreversal, the cross-link photoreversal is preferentially at the pyrone end at all wavelengths. At this pH the k_2/k_1 ratios are slightly reduced at longer wavelengths. This is the reverse of that observed for the closed form of the diadduct. Identical k_2/k_1 ratios were obtained for the cross-link at both pH 5.5 and pH 7.5 (data not shown). Consequently, it is assumed that the closed form of the cross-link is the only species at pH 7.5. These results infer that the DNA helix alters the chemistry of the photoreversal. A diadduct in a DNA helix would be expected to be more resistant to pyrone ring opening because of charge repulsion between the phosphates and the additional negative charge formed upon ring opening. Therefore, photoreversal at even higher pH was performed. Samples of cross-link solution at pH 10.0 (20 mM borate buffer) were incubated at 60 °C for 2 h and photoreversed. The samples were then acidified to ca. pH 5, EtOH-precipitated with carrier tRNA, and analyzed by gel electrophoresis. Similar experiments were done at pH 12.0 (20 mM phosphate buffer) except that the cross-link solution was kept at room temperature for 4 h instead of incubating at 60 °C. Control samples showed that there is a negligible amount of damage to the cross-link at these high pH conditions. From the results in Table I, it is apparant that the k_2/k_1 ratio increases at all wavelengths as the pH of the photoreversal solution increases. Again it is consistent with the idea that photoreversal of the pyrone-ring-opened form of the cross-link yields only the pyrone-side monoadducted DNA. In contrast to the diadduct photoreversal, the k_2/k_1 ratio for the cross-link photoreversal at 249 nm does increase when the pH increases. At these high pHs, different mechanisms may be contributing to the photoreversal of the cross-link compared to that of the diadduct.

DISCUSSION

Quantum Yield of the Diadduct Photoreversal. The extinction spectrum of the diadduct in Figure 7 clearly shows

that there are at least two absorption bands in the wavelength region 240–350 nm. There is a pronounced absorption band that is centered at about 290 nm and a very large shoulder that continues to rise for wavelengths less than 270 nm. The action spectrum for photoreversal of the diadduct is also shown in Figure 7 for comparison. The action spectrum is analogous in shape to the absorption spectrum of the diadduct. There is a peak in photoreversal at 290 nm and a shoulder that rises in parallel with the absorption spectrum at wavelengths less than 270 nm. Calculation of the quantum yield for photoreversal from the data of Figure 7 also indicates that two distinct absorption bands contribute to photoreversal. Below 280 nm, the quantum yield is a constant value of 0.16 ± 0.04. Above 280 nm, the quantum yield is about twice as large (0.30 ± 0.04) and again appears to be constant within the wavelength region 289–313 nm. Thus, we conclude that photoreversal can be effected through two distinct absorption bands. In analogy with pyrimidine dimer photoreversal, it is likely that excitation of the adducted pyrimidines leads to photoreversal of the psoralen–pyrimidine diadducts, particularly at wavelengths below 280 nm. The quantum yield for photoreversal of a psoralen–pyrimidine diadduct in this wavelength region is much smaller than the quantum yield for photoreversal of a pyrimidine dimer, which is about unity (Deering & Setlow, 1963). Both electronic and steric factors may contribute to this difference in quantum yields.

Effects of Local Helical Structure and Adjacent Bases. The action spectra for photoreversal of the diadduct and cross-link are compared in Figure 5. The wavelength dependence for the sum of the rate constants ($k_1 + k_2$) for both the diadduct and cross-link is almost identical at wavelengths above 290 nm. However, the cross-linked DNA photoreverses more efficiently at wavelengths between 240 and 290 nm than does the isolated diadduct. Several factors may contribute to this enhancement of the rates of photoreversal. The absorption spectrum of the diadduct may be different in a DNA helix compared to the free diadduct. It is not possible to measure the absorption spectrum of the diadduct in a helix because of hyperchromic effects of the adjacent DNA bases and the unknown deformation created by a diadduct in the helix. The photoreversal enhancement may also reflect a true quantum yield difference induced by increased strain of the cyclobutane bridges when the diadduct is incorporated into a helix. If this were contributing significantly, we would expect to see an equal enhancement at wavelengths above 290 nm. Since the photoreversal rate constants are about equal above 290 nm, we do not belive that we are observing an increase in quantum yield for a reversal reaction. A third source of photoreversal enhancement is energy migration from excited DNA bases to the diadduct. The shape of the difference of the two action spectra of Figure 5 is similar to the absorption spectra of DNA. The wavelength dependence for the enhancement we have observed is thus consistent with absorption by DNA bases.

Selective Production of Monoadducts. Photoreversal of a diadduct or cross-link yields two types of monoadducts or monoadducted oligonucleotides. The data in Table I show that the pyrone-side monoadduct is the major product of the diadduct photoreversal, whereas the furan-side monoadducted oligonucleotide is the major product of the cross-link photoreversal. It is clear that the local structure of the DNA helix adjacent to a diadduct affects the photochemistry of the reversal reaction.

The selective production of monoadducts is highly dependent on the pH of the solution. From the results in Table I, we proposed a mechanism for the photoreversal of both the di-
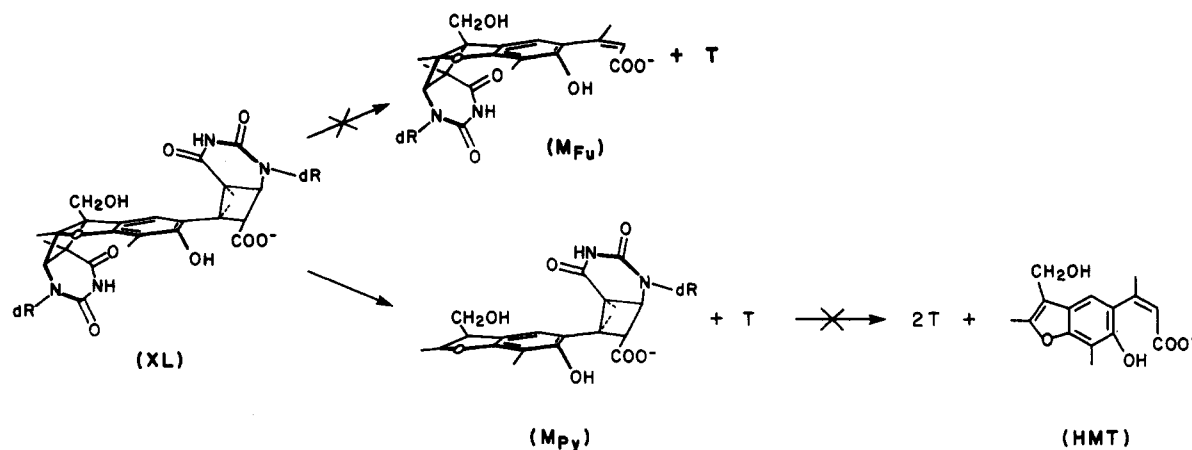
FIGURE 9: Photoreversal of the pyrone-ring-opened diadduct (or cross-link). T stands for free thymidine or DNA.

Table II: Cross Sections of DNA–HMT Cross-Link Photoreversal and Nucleic Acid Photodamages ($\times 10^{-19}$ cm^2/Quanta Base)

photochemical event	wavelength (nm)							source
	240	254	265	280	290	302	313	
photoreversal of DNA–HMT cross-link	229	139	91.3	49.0	29.1	10.1	0.92	data of Figure 5
single-strand break formation in cells	1.2×10^{-4}	2.3×10^{-4}	3.2×10^{-4}	2.3×10^{-4}	1.0×10^{-4}	1.3×10^{-5}	3.1×10^{-6}	Rosenstein & Ducore (1983)
single-strand break formation in bacteria		2.1×10^{-3}	9.2×10^{-4}	2.1×10^{-4}		2.0×10^{-5}	5.1×10^{-6}	Peak & Peak (1982)
T⌒T dimer formation in poly(dT)	9.9	20	19	8.8				Deering & Setlow (1963)
U⌒U dimer formation in poly(rU)	3.90	7.97	7.32	1.52	0.40			Pearson et al. (1966)
U hydrate formation in poly(rU)	1.49	3.65	4.12	1.44	0.20			Pearson et al. (1966)
T⌒T dimer formation in cells		1.68	1.35	1.08	0.67	3.8×10^{-2}	6.8×10^{-4}	Rothman & Setlow (1979)

adduct and cross-link at high pH. This is shown in Figure 9. At low pH, the pyrone-ring-closed form of the diadduct or cross-link is predominant. The pyrone ring of the adduct opens as the pH increases (Figure 9), shifting the equilibrium to the open forms. Photoreversal of the pyrone-ring-opened diadduct or cross-link at the pyrone side is blocked because of the loss of the conjugation between the pyrone ring and the benzene ring. Consequently, only pyrone-side monoadduct or pyrone-side monoadducted DNA is produced upon photoreversal. The pyrone-side monoadduct or pyrone-side monoadducted DNA is resistant to further photoreversal for the same reason. There is, however, still a difference between the diadduct and the cross-link. At 249 nm, the ratio of k_2/k_1 for the diadduct is insensitive to the pH change, whereas this same ratio for the cross-link increases when the pH of the solution goes up. To explain this observation, we proposed that the diadduct photoreversal at 249 nm is predominantly due to the absorption of the adducted thymidine group. Therefore, the ring opening has no effect on the k_2/k_1 ratio and on the further photoreversal of the monoadducts. On the other hand, it is possible that the photoreversal of the cross-link at 249 nm is caused in part by energy transfer from adjacent bases to the psoralen moiety of the cross-link. This is supported by the enhanced photoreversal rate constant ($k_1 + k_2$) at wavelengths below 290 nm for the cross-link compared to the isolated adduct. Consequently, photoreversal is still sensitive to the pyrone ring opening, since photoreversal is effected through excitation of the benzene group of the parent psoralen.

The ability to selectively photoreverse one of the two cyclobutane rings of a cross-link in DNA might allow for the site-specific placement of a psoralen molecule within a large RNA or DNA. The site-specific placement procedure would

be a three-step process. First, a monoadducted oligonucleotide with a psoralen attached at a specific pyrimidine and in a specific orientation (either furan-side monoadduct or pyrone-side monoadduct) must be generated. An oligonucleotide with these characteristics can be easily obtained by following the procedures described in this paper. Second, the monoadducted oligonucleotide would be hybridized to its complement in a large DNA or RNA and subsequently cross-linked. The cross-lined complex would then be photoreversed under conditions which favor retention of the psoralen on the larger RNA or DNA molecule. The monoadducted RNA or DNA could then be used for secondary and tertiary structure analysis by reirradiating to form intramolecular cross-links site specifically in the RNA or DNA. If this latter goal is to be achieved, it would be best to start with a pyrone-side monoadducted oligonucleotide. The psoralen transferred to the larger RNA or DNA as a monoadduct would then be of the furan-side type, which is favored upon photoreversal and easily cross-linked by exposure to 320–400-nm light. The transfer procedure just described has two drawbacks. First, a pyrone-side monoadduct must be driven to cross-link. We have preliminary evidence that demonstrates that a pyrone-side monoadducted oligonucleotide is cross-linkable when it is irradiated (≥ 320 nm) in the presence of a suitable triplet sensitizer such as triphenylene (G. Cimino and Gartenberg, unpublished observations). The second drawback is the exposure of the cross-linked oligonucleotide/DNA (or RNA) complex to photoreversal light. Since the action spectrum for photoreversal of a psoralen cross-link overlaps with nucleic acid absorption spectrum, there will certainly be some damage introduced into the larger DNA or RNA of the cross-linked complex. To estimate the potential damage created by a

photoreversal step, we have calculated the cross sections for photoreversal (see eq 24 in the supplementary material). These are listed in Table II along with the cross sections of several types of nucleic acid UV damage.

It is seen from Table II that, in both the bacteria and eucaryotic cells, the single-strand breaks represent only a minor form of damage. (These cross sections cm^2/quanta base were derived from the our original data.) All the nucleic acid UV damage cross sections decrease faster than the photoreversal cross section of the cross-link as the irradiation wavelength increases. Therefore, UV damage to nucleic acids can be minimized by photoreversing psoralen nucleic acid cross-links at longer wavelengths, e.g., 313 nm. Another kind of DNA damage that is not listed in Table II is the formation of monomeric thymine ring saturation products. These products are as large as 73% of the thymidine dimer formed at 313 nm (Hariharan & Cerutti, 1977). When all the nucleic acid UV damage cross sections are combined together (including monomeric thymine saturation products), it is estimated that photoreversing one cross-link at 313 nm will cause one photodamage per ca. 600 bases of nucleic acid. This level of damage can be tolerated when the secondary structure of an RNA molecule of the size of 23S rRNA or smaller is analyzed.

CONCLUSION

In this paper, we reported the action spectra for the photoreversal of both the T–HMT–T diadduct and HMT-KpnI linker DNA cross-link. We also show that we can minimize photodamage to nucleic acids by photoreversing psoralen cross-links at 313 nm. We presented the dramatic effect of the DNA double helix on both the total rate constants ($k_1 + k_2$) and the ratio of k_2/k_1 of the photoreversal. The ratio of k_2/k_1 is also highly dependent on the irradiation wavelength and the pH of the solution. Finally, we proposed mechanisms for photoreversal at different solution conditions and describe a procedure for the site-specific placement of a psoralen molecule into a large DNA or RNA.

SUPPLEMENTARY MATERIAL AVAILABLE

A detailed derivation of the kinetic equations for cross-link and diadduct photoreversal and a derivation of the relationship between the rate constant ($k_1 + k_2$) and the reaction cross section ($\sigma_1 + \sigma_2$) (3 pages). Ordering information is given on any current masthead page.

Registry No. HMT, 62442-59-5; T–HMT–T, 101418-62-6.

REFERENCES

Ben-Hur, E., & Song, P. S. (1984) Adv. Radiat. Biol. 11, 131–171.

Cassier, C., Chanet, R., & Moustacchi, E. (1984) Photochem. Photobiol. 39, 799–803.

Cimino, G. D., Gamper, H. B., Isaacs, S. T., & Hearst, J. E. (1985) Annu. Rev. Biochem. 54, 1151–1193.

Deering, R. A., & Setlow, R. B. (1963) Biochem. Biophys. Acta 68, 526–534.

de Mayo, P., & Shizuk, H. (1976) in Creation and Detection of the Excited State (Ware, W. R., Ed.) Vol. 4, pp 164–182, Marcel Dekker, New York, Basel.

Fitzpatrick, J. B., Stern, R. S., & Parrish, J. A. (1982) in Psoriasis—Proceedings of the 3rd International Symposium (Farber, E. M., Ed.) pp 149–156, Grune and Stratton, New York.

Fujita, H. (1984) Photochem. Photobiol. 39, 835–839.

Gamper, H., Piette, J., & Hearst, J. E. (1984) Photochem. Photobiol. 40, 29–34.

Garrett-Weeler, E., Lockard, R. E., & Kumar, A. (1984) Nucleic Acids Res. 12, 3405–3423.

Gasparro, F. P., Saffron, W. A., Cantor, C. R., & Edelson, R. L. (1984) Photochem. Photobiol. 40, 215–219.

Hariharan, P. V., & Cerutti, P. A. (1977) Biochemistry 16, 2791–2795.

Hearst, J. E., Isaacs, S. T., Kanne, D., Rapoport, H., & Straub, K. (1984) Q. Rev. Biophys. 17, 1–44.

Isaacs, S. T., Shen, C.-K. J., Hearst, J. E., & Rapoport, H. (1977) Biochemistry 16, 1058–1064.

Isaacs, S. T., Rapoport, H., & Hearst, J. E. (1982a) J. Labelled Compd. Radiopharm. 19, 345–356.

Issacs, S. T., Chun, C., Hyde, J. E., Rapoport, H., & Hearst, J. E. (1982b) In Trends In Photobiology (Helene, C., Charlier, M., Monternay-Carestier, Th., & Laustriat, G., Eds.) pp 279–294, Plenum, New York.

Kanne, D., Straub, K., Hearst, J. E., & Rapoport, H. (1982a) J. Am. Chem. Soc. 104, 6754–6764.

Kanne, D., Straub, K., Rapoport, H., & Hearst, J. E. (1982b) Biochemistry 21, 861–871.

Maniatis, T., Fritsch, E. F., & Sambrook, J. (1982) in Molecular Cloning, pp 125–126, Cold Spring Harbor Laboratory, Cold Spring Harbor, NY.

Parsons, B. J. (1980) Photobiochem. Photobiol. 32, 813–821.

Peak, M. J., & Peak, J. G. (1982) Photobiochem. Photobiol. 35, 675–680.

Pearlman, D. A., Holbrook, S. R., Pirkle, D. H., & Kim, S. H. (1985) Science (Washington, D.C.) 227, 1304–1308.

Pearson, M., Whillans, D. W., LeBlanc, J. C., & Jones, H. E. (1966) J. Mol. Biol. 20, 245–261.

Peckler, S., Graves, B., Kanne, D., Rapoport, H., Hearst, J. E., & Kim, S. H. (1982) J. Mol. Biol. 162, 157–172.

Rosenstein, B. S., & Ducore, J. M. (1983) Photobiochem. Photobiol. 38, 51–55.

Rothman, R. H., & Setlow, R. B. (1979) Photobiochem. Photobiol. 29, 57–61.

Saffran, W. A., & Cantor, C. R. (1984) J. Mol. Biol. 178, 595–609.

Song, P. S., & Tapley, K. J., Jr. (1979) Photobiochem. Photobiol. 29, 1177–1197.

Straub, K., Kanne, D., Hearst, J. E., & Rapoport, H. (1981) J. Am. Chem. Soc. 103, 2347–2355.

Thompson, J. F., & Hearst, J. E. (1983) Cell (Cambridge, Mass.) 32, 1355–1365.

Turner, S., & Noller, H. F. (1983) Biochemistry 22, 4159–4164.